

Thermal shock behaviour of unidirectional silicon carbide fibre reinforced calcium aluminosilicate

M. J. BLISSETT*, P. A. SMITH, J. A. YEOMANS

Department of Materials Science and Engineering, University of Surrey, Guildford, Surrey GU2 5XH, UK

Unidirectional silicon carbide fibre-reinforced calcium aluminosilicate (CAS) has been subjected to a variety of thermal regimes. Microscopy has been used to assess the degree of matrix damage. Thermal shock induced matrix cracking was first seen on the end faces of the composite, perpendicular to the fibre direction at a temperature differential of 400 °C. At more severe thermal shocks the next damage was observed on faces parallel to the fibre direction in the form of cracking in the matrix perpendicular to the fibre direction. Matrix cracking damage increased, initially, with increasing severity of thermal shock, but then became less extensive at the highest temperature differentials (800 °C) used. Thermal shock-induced crack densities were correlated with literature data for cracking under quasi-static loading using a simple thermal shock analysis incorporating a stress reduction factor. The suitability of applying a modified Aveston, Cooper and Kelly (ACK) model [1] to predict critical temperature differentials for matrix cracking onset in the unidirectional composite has also been tested. The method was found to be valid for the unidirectional material providing that some key parameters were determined independently.

1. Introduction

The efficiency of gas turbine engines is governed by the maximum operating temperature, hence there is a desire to increase the elevated temperature capability of the turbine components. One class of materials that may be suitable for use at high temperature is continuous fibre-reinforced ceramic matrix composites (CMCs). Room temperature properties and mechanical behaviour of these composites, notably the early model systems of silicon carbide fibre-reinforced lithium aluminosilicate (LAS) and calcium aluminosilicate (CAS), have been studied extensively [2–4] and two areas that have received particular attention are the introduction of matrix cracks [5–9] and the role of the interphase [10–14].

Applications in high temperature environments will inevitably involve an element of thermal cycling where components will be subjected to rapidly changing stress states and thus, thermal shock damage. There are few reports of research on ceramic matrix composites in this topic area [15] although some work has been undertaken on elevated temperature performance [3, 16–18] and residual properties after thermal ageing [13, 19–21]. In the present work the effect of thermal shock on unidirectional Nicalon reinforced CAS is assessed and the possibility of using the model of Aveston *et al.* [1] to predict maximum operating temperatures is explored.

2. Materials

The glass ceramic composite used in this study consisted of a matrix of calcium aluminosilicate (CAS), identified as stoichiometric $\text{CaO-Al}_2\text{O}_3-2\text{SiO}_2$ containing a fine dispersion of ZrO_2 (probably as a nucleating agent) reinforced with tows of continuous SiC (Nicalon) fibres. This material (supplied by courtesy of Rolls-Royce plc) was prepared by hot pressing 12 plies of unidirectionally stacked “pre-preg” to form a sheet approximately 2.3 mm thick. The fibres were nominally 15 μm in diameter and had a fibre volume fraction of approximately 0.34, although wide local variations were apparent. Samples of monolithic CAS were also supplied for use in the experimental programme. Table I summarises some of the properties of the materials.

3. Experimental procedures

Samples of both materials were cut from plates using a high speed diamond saw and then polished carefully on three orthogonal faces to a high quality finish. At least 300 μm of material was removed from sawn faces to remove any damage caused by the cutting process to give final dimensions of $10 \times 2.2 \times 2.2$ mm for both materials, plus larger samples ($10 \times 10 \times 2.2$ mm) of the composite.

Thermal treatments were carried out using an electric muffle furnace. Samples were checked by reflected

* Current address: Department of Materials, Queen Mary and Westfield College, Mile End Road, London E1 4NS, UK

TABLE I Properties of constituents of the composite material

E_f	fibre modulus	190 GPa
α_f	fibre thermal expansion coefficient	$3.3 \times 10^{-6} \text{ K}^{-1}$
E_m	matrix modulus	90 GPa
α_m	matrix thermal expansion coefficient	$4.6 \times 10^{-6} \text{ K}^{-1}$
V_f	fibre volume fraction	0.34

light microscopy (RLM) to ensure that the polished faces were free from any preparation damage, and then placed on an upturned alumina crucible and inserted into the muffle furnace that had been allowed to equilibrate at a pre-determined temperature (it was found that the rate of temperature change in the sample caused by this method had no deleterious effect on the material properties). After a pre-determined time had elapsed either the furnace was turned off and the samples allowed to cool in the furnace (thermal ageing experiments) or the crucible was removed from the furnace and the samples plunged rapidly into a large quantity ($> 10\text{ l}$) of water at a temperature of 20°C (thermal shock experiments).

Observations of the surfaces of the samples were performed primarily by reflected light microscopy. After exposure to thermal regimes, some of the larger samples were progressively ground back perpendicularly to the fibre direction to investigate the sub-surface crack profile. To enhance the contrast between the material and the cracks, some samples were immersed in an aqueous solution of silver nitrate for 30 min and dried prior to observation. Higher magnification imaging was achieved by carbon coating the samples and then viewing by scanning electron microscopy (SEM).

4. Thermal ageing effects

In order to separate effects due to thermal shock from thermal ageing alone, samples of both the monolithic and composite material were exposed to elevated temperatures for extended periods and allowed to cool slowly in the furnace.

Samples were placed into the furnace at pre-set temperatures and for all thermal ageing temperatures (up to 800°C) there was no evidence of any cracks on the surface of the monolithic CAS. Samples of the composite, aged between $500\text{--}800^\circ\text{C}$ and maintained at that temperature for periods between $1\text{--}150\text{ h}$ also showed no evidence of cracking on the surfaces of the specimens. However, when viewed by RLM the most noticeable feature on the surface of the composite was the debonding of fibres from the matrix and for higher temperatures and/or longer duration heat treatments this phenomenon became more pronounced as exhibited by the increased frequency of debonds primarily in, or adjacent to, matrix-rich areas. Examination by SEM and topographical analysis using confocal laser scanning microscopy (CLSM) revealed that some of these debonded fibres protruded in excess of $1\ \mu\text{m}$ above the surface of the composite.

A second effect, particularly evident after high temperature heat treatment, was the covering of appar-

ently randomly selected areas of the surface of the cross-sectional plane of the composite by a layer of nominally transparent material.

5. Observations of cracking damage

5.1. Monolithic CAS

Thermal shocks with a temperature differential (ΔT) of 500°C or greater applied to the samples produced a network of cracks over the entire surface. For thermal shocks below this value the density of cracks reduced until at ΔT of 360°C only one or two cracks were visible on the polished faces and with $\Delta T = 350^\circ\text{C}$ no cracks were observed, hence the onset of cracking was considered to be at a temperature differential of 360°C .

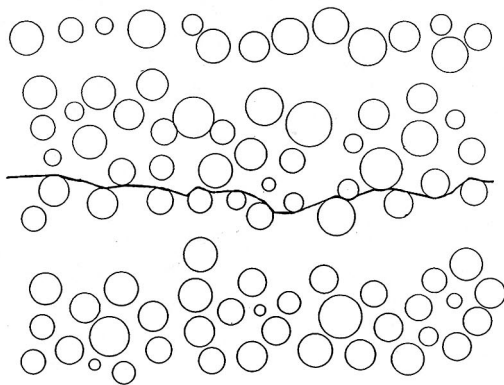
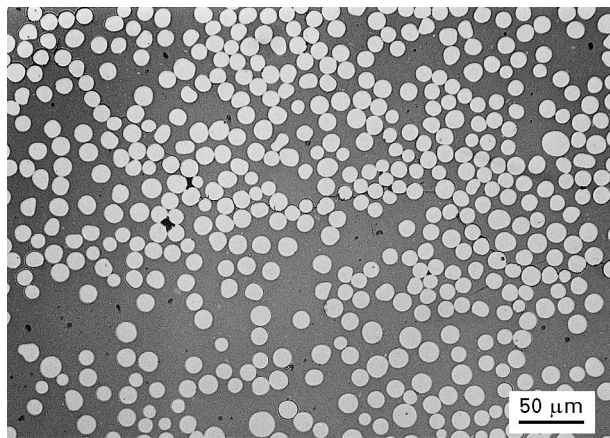
5.2. Unidirectional Nicalon/CAS

5.2.1. Perpendicular to fibre direction

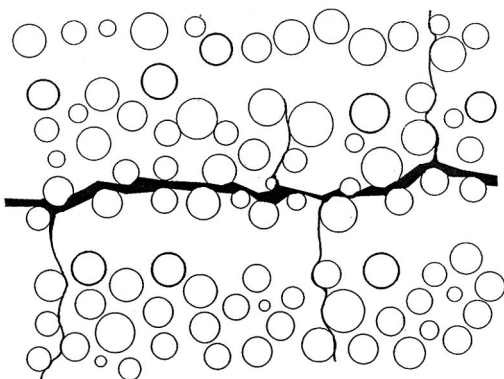
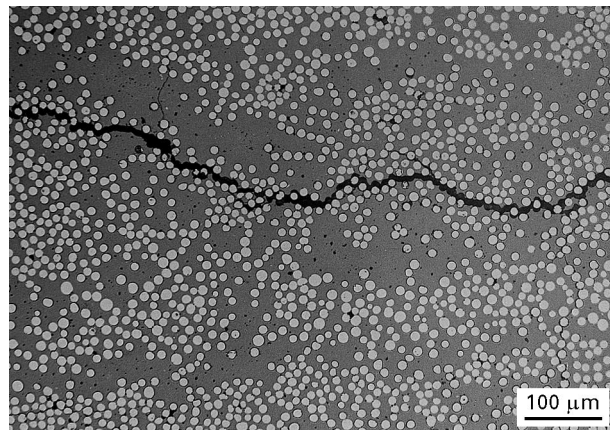
The initial experiments were conducted on the large samples soaked at elevated temperatures for 1 h. For temperature differentials below 300°C there was no discernible change in the sample; at greater temperature differentials there was evidence of fibre debonding and at 400°C a single, fine crack was observed. This crack traversed most of the polished surface, centrally between the two large faces, and was contained in a fibre-rich area. On increasing the severity of the downward thermal shock the crack opening displacement increased, approaching one fibre diameter at 800°C . At these elevated temperatures the introduction of fine, random cracks perpendicular to the major axis was also evident (Fig. 1a and b). After material had been removed during subsequent grinding stages, observations and measurements indicated that the major crack profile was approximately semicircular and emanated from the centre of the polished surface. The more severe thermal shocks generated cracks which traversed the whole length of the original surface and penetrated several millimetres into the end of the sample, whilst the small, perpendicular cracks did not extend more than $300\ \mu\text{m}$ into the bulk of the material. A reduction in the cross-sectional area to a square profile had no discernible effect on the crack pattern.

Extending the time for which the samples were held at the elevated temperature appeared to lead to a reduction in the degree of cracking caused by the subsequent thermal shock, e.g., the appearance of the crack produced after thermal ageing samples for 60 h and then thermal shocking from a temperature differential (ΔT) of 600°C was similar to that of samples thermally aged for 1 h prior to shocking with a ΔT of 500°C . However, from the limited number of examples investigated, it appears that the maximum effect of the longer soak is attained within a few hours and does not reduce the crack width to less than that commensurate with a thermal shock produced by a ΔT of $50\text{--}100^\circ\text{C}$ lower.

Observations on samples that had been thermally aged at 400°C for 1 h and then thermally shocked



(a)



(b)

Figure 1 Reflected light photomicrographs and schematics of cracks in unidirectional Nicalon/CAS produced by thermal shock with (a) $\Delta T = 450^\circ\text{C}$ and (b) $\Delta T = 800^\circ\text{C}$.

TABLE II Crack densities and matrix axial stresses of thermally shocked unidirectional Nicalon/CAS (mechanical data taken from reference [7])

Temp. diff. ΔT ($^\circ\text{C}$)	400	450	500	600	700	800	840	880
Crack spacing (mm)	5.00	5.00	0.64	0.39	0.29	0.26	0.33	0.40
Crack density (mm^{-1})	0.20	0.20	1.56	2.58	3.40	3.92	3.06	2.50
Tot stress (th) ($A = 0.5$) (MPa)	167	178	188	209	229	250	258	266
Total stress ^a (mech) (MPa)	146	146	195	208	215	219	212	207

^a This assumes a residual matrix axial stress of 80 MPa

indicated that debonding of fibres occurred in fibre-rich areas of the surface of the composite. Series of single debonds appeared to be connected in an almost “string-like” manner of varying orientation. As the severity of the thermal treatment increased the degree of debonding in the fibre-rich areas reduced greatly until at high temperatures (e.g., 800°C) these areas were devoid of any apparent debonds. However, at temperatures above 600°C , debonding in matrix-rich regions became evident. These debonds were predominantly of isolated fibres within the matrix although fibres bordering fibre-rich regions were also affected.

5.2.2. Parallel to fibre direction

Observations of the large surfaces of a range of samples thermally aged and quenched after 1 h from temperature differentials (ΔT) below 400°C suggested that such cycles did not lead to any surface cracks. For thermal shocks with a temperature differential of 400°C the large face exhibited a few cracks of various orientations; some went through the matrix and were perpendicular to the major fibre axis whilst others appeared to follow the contours of sub-surface fibres. As the severity of the thermal shock increased the spacing between the perpendicular matrix cracks was seen to vary as shown in Table II.

6. Discussion

6.1. Thermal ageing

The lack of any cracks on the surfaces of both the monolithic and composite materials after samples were cooled slowly confirms that thermal shock was the cause of cracking. Debonding of the fibres in the composite was commensurate with a relaxation of the residual processing stresses during the heating cycle and the ingress of oxygen down the interphase must be considered to be involved in promoting this debonding by an oxidative process leading to a reduction in interfacial shear strength.

The appearance of the glassy film over the cross-sectional surface of the composite is possibly as a consequence of the removal of the carbon interphase allied with oxidation of the silicon carbide. Since the specific volume of silica is almost twice that of carbon then the silica is likely to exude out of the interphase

and over the surface. It has been suggested that short, high temperature thermal excursions may be successful in providing protection against embrittlement by sealing the surfaces of components prior to use at elevated temperatures [21, 22].

6.2. Cracking due to thermal shock

6.2.1. Monolithic CAS

The conversion of critical temperature differential to an applied stress generated by an infinitely fast quench has been calculated from a simple relationship [23]:

$$\sigma_{ts} = \frac{\Delta TE\alpha}{(1 - \nu)} \quad (1)$$

From the manufacturer's figures an average value for the Young's modulus of the matrix, (E_m), is 90 GPa, the coefficient of thermal expansion of the matrix, (α_m), is $4.6 \times 10^{-6} \text{ K}^{-1}$ and Poisson's ratio, (ν), is 0.25 giving the stress due to thermal shock from 380 °C as 200 MPa. However, this quench rate is unrealistic and, in a more rigorous approach [23], another parameter, A , was introduced. This modified Equation 1 to:

$$\sigma_{ts} = \frac{A\Delta TE\alpha}{(1 - \nu)} \quad (2)$$

The quantity, A , termed a "non-dimensional stress reduction factor" is a function of the Biot modulus, β which is given by $\beta = ah/k$ with the term "a" being a characteristic dimension of the sample under consideration, h is the heat transfer coefficient of the quenching medium and k , the thermal conductivity of the sample. There will be no benefit derived from using this more complex expression unless the terms which make up β and hence A , can be evaluated accurately. However, disagreements between theory and experiment, and the variability in experimental results themselves, are often attributed to the difficulty in evaluating the Biot modulus [24, 25].

Davies *et al.* [26] performed a series of three-point flexure tests on a monolithic CAS material and obtained a mean value for the bend strength of 290 MPa and a Weibull modulus of 5.4. Using a very simple approach the relationship between ultimate tensile strength (UTS) and bend strength (MOR) can be given as:

$$\frac{MOR}{UTS} = [2(m + 1)^2]^{1/m} \quad (3)$$

Assuming comparable sample volumes, the bend strength can be converted into a tensile strength value of 128 MPa leading to a value for the stress reduction factor (A) for monolithic CAS of 0.64.

6.2.2. Unidirectional Nicalon/CAS

6.2.2.1. *Perpendicular to fibre direction.* The observed pattern of cracks is different from the arrangement that would be expected in a monolithic ceramic in which cracks tend to grow inwards from the surfaces [27]. Possible reasons for this difference in behaviour

have been considered. On the macroscopic level the material can be described as a layered structure of alternate fibre and matrix rich planes. These have different elastic and thermal properties and hence respond differently to thermal shock, which may give rise to either a peeling or sliding effect. On a microscopic scale tensile matrix hoop stresses exist around the fibres at the surface of the material as a result of the mismatch in coefficients of thermal expansion. These are greater than the axial or radial stresses and increase in magnitude with increasing fibre volume fraction [28]. These microscopic stresses are superimposed onto the macroscopic stresses giving rise to a through-thickness stress which is greater than stresses in other directions.

For a thermal shock with a temperature differential of 400 °C the magnitude of the thermally generated stress in the matrix can be estimated, using Equation 2, to be 110 MPa; assuming a value for the stress reduction factor for the matrix in the composite to be 0.5 (see below for determination of stress reduction factor in Nicalon/CAS composite). The residual stress within the composite is more difficult to determine, however, since it comprises matrix hoop and radial stresses. From the model of Powell *et al.* [28], which assumes that the composite is stress free at the processing temperature of 1200 °C, the maximum tensile hoop stress in the bulk of the material at room temperature for a fibre volume fraction of 0.34 will be 130 MPa, and the compressive radial stress will be 65 MPa. If a representative value of residual tensile stress across the path taken by the crack is 100 MPa at room temperature, then this will be reduced to 65 MPa at a furnace temperature of 420 °C, giving a total stress of 175 MPa at the initiation of cracking.

The maintenance of a similar crack pattern after the reduction in size to cuboids suggests that differential heat loss between large and small faces is not a controlling factor. The results indicated that a change in crack path geometry was observed with increasing severity of thermal shock. This effect may arise as a consequence of changing interfacial shear strength and dynamic crack growth. At low temperature (400 °C) there will be a relatively small driving force for crack growth and little change to the interface. The crack is likely, therefore, to follow the weak interface between the fibre and matrix until the magnitude of the residual hoop stresses, due to the close proximity of an adjacent fibre, provides a favourable path for the crack to proceed. As the severity of the thermal treatment increases the interface will become weakened (due to the oxidation of carbon), the envisaged peeling/sliding stresses will increase and crack propagation will be more energetically favourable. Since the increase in applied stress will be greater than the reduction in interfacial shear strength the overall combined effect of these changes will be to promote linear crack growth. The formation of silica bridging at the highest temperatures used in this study would be expected to strengthen the interface and to enhance, further, the straightening of the crack path. Hence at more severe thermal shocks the crack path is noticeably less interfacial.

Debonding of the fibres from the matrix was a feature common to all thermal regimes to a lesser or greater extent. Debonding during the thermal ageing process will be associated with changes to the structure of the interface, resulting from the oxidation of carbon. Additionally, during the thermal shock process, there may be a partial release of the clamping residual radial matrix stresses associated with minor cracking events in the vicinity of the fibre.

6.2.2.2. Parallel to fibre direction. The results indicated a minimal effect on samples shocked below 400 °C, a steep increase in matrix crack density between 500–800 °C, then a decrease above this temperature. The low temperature results can probably be explained by noting that the severity of the thermal shock was not sufficient to cause multiple cracks. The occurrence of cracks associated with the sub-surface fibres was probably due to tensile matrix hoop stresses generated around fibres when the composite cooled. Powell *et al.* [28] calculated these stresses to be in excess of 100 MPa at room temperature; these will decrease with distance into the matrix from the fibre but any fibres sufficiently close to the free surface will render the matrix susceptible to cracking. Matrix cracks have also been observed in thermally shocked unidirectional reinforced Nicalon/LAS composites [15] but, since the matrix hoop stresses will be compressive for this system, they concluded that the cracking was due to thermal expansion anisotropy of a crystalline phase formed in the matrix at elevated temperatures.

The large increase in crack density at intermediate temperatures is partially due to greater thermal stresses induced by the thermal shock. The effect of increased temperature also causes oxidation of the exposed interfacial carbon and this reduces the interfacial sliding resistance [13], thus negating benefits that may have been derived from the reinforcing fibres. This effect is shown in Fig. 2 where the interfacial bonding between fibres and matrix is too weak to prevent the matrix from cracking around the fibres.

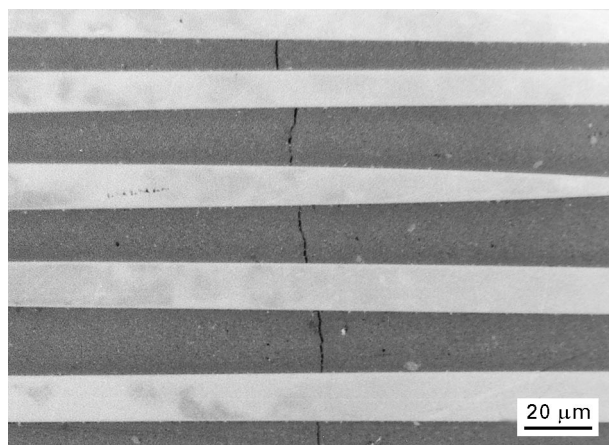


Figure 2 Reflected light photomicrograph showing fibre debonding and matrix cracking in unidirectional Nicalon/CAS after thermal shock with $\Delta T = 500$ °C.

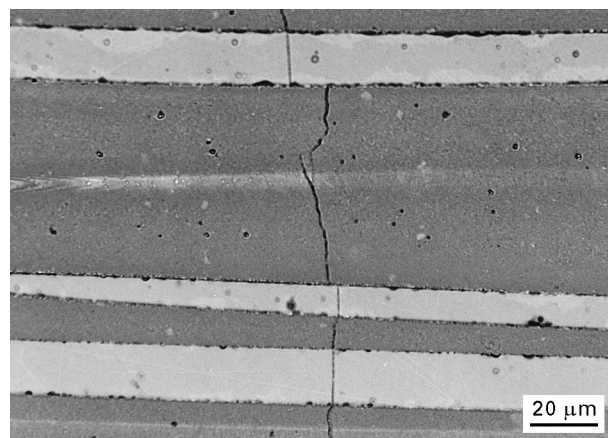


Figure 3 Reflected light photomicrograph showing fibre fracture and matrix cracking in unidirectional Nicalon/CAS after thermal shock with $\Delta T = 800$ °C.

The observed reduction in the effect of the shock at the highest temperatures is commensurate with the formation of strong, silica bridging between the matrix and the fibres. This strong, but brittle interphase increases the sliding resistance sufficiently to render the composite notch-sensitive so that when matrix cracking does occur the fibres are also fractured (Fig. 3).

The onset of matrix cracking is apparent at a ΔT of approximately 400 °C. An important feature, which is absent in the monolithic material, is the residual stress introduced into the composite during the fabrication process. Calculations have been performed to determine the values of the residual matrix stresses parallel to the fibres using the model of Powell *et al.* [28] and these values are added to the values of the applied thermal stresses due to the thermal shock process, calculated from Equation 1, to give a total matrix stress. For a temperature differential of 400 °C the residual tensile stress is calculated to be 57 MPa (this assumes a stress-free processing temperature of 1200 °C) and the applied stress for an infinitely fast quench is 222 MPa giving a total stress of 279 MPa.

From reports [6, 7, 28] an average value for residual matrix axial stress may be taken as 80 MPa. A value for the applied stress to initiate matrix cracks at room temperature can also be determined from representative literature values for mechanically applied composite stresses. A typical value quoted for composite stress is 120 MPa [6, 7]. By using the constant strain relationship ($\sigma_m = \sigma_c E_m / E_c$), where σ is applied stress, E is Young's modulus and m and c refer to matrix and composite respectively, the applied matrix axial stress required to initiate matrix cracking becomes 87 MPa; giving a total matrix stress of 167 MPa. The calculated value of 279 MPa for the total matrix stress is high but of course this calculation assumes an infinitely fast quench. The total stress to initiate a crack in the matrix should be the same whether applied thermally or mechanically. Residual stresses will obviously remain in the material but at 420 °C these are reduced to 57 MPa and, if Equation 2 is used, the applied thermal stress in the matrix can be reduced to approximately 110 MPa by giving "A" the value 0.5, and the total

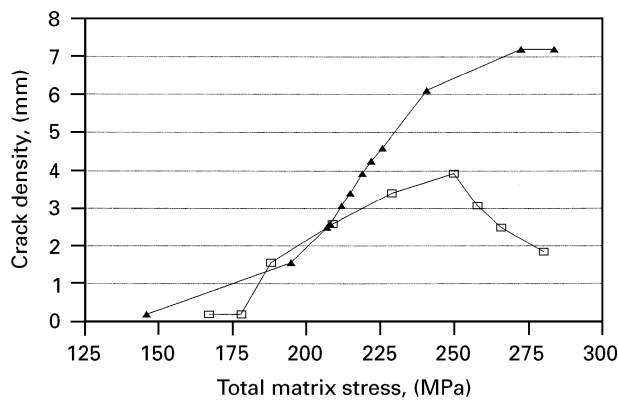


Figure 4 Comparison of crack densities as a function of matrix axial stresses generated, (▲) mechanically or (□) thermally in unidirectional Nicalon/CAS.

stress then becomes 167 MPa, matching the mechanical stress value. This assumed value for A is not unreasonable since the thermal conductivity of the silicon carbide fibres is expected to be higher than for the monolithic CAS. The same procedures can be followed to obtain the stresses associated with the crack density measurements of Table II. These matrix axial stress values are compared with the matrix stress values calculated from the data of Pryce and Smith [7] for crack densities as a function of composite stress on the same material when subjected to mechanical tensile stresses at room temperature. Comparison of the two complete sets of results (Fig. 4) indicate quite good correlation between crack densities and total matrix axial stresses below 210 MPa. At higher levels of stress the crack density continues to increase up to a plateau of 7 mm^{-1} for the mechanically applied loads whereas, cracks due to thermal stresses reach a peak of 4 mm^{-1} at 250 MPa before reducing beyond this level of matrix stress.

This effect is consistent with the changing interfacial properties of the composite with temperature. Crack density measurements of between $1.5\text{--}2.5 \text{ mm}^{-1}$ are associated with thermal shock temperature differences of $500\text{--}600^\circ\text{C}$. At these temperatures it is conjectured that the interface is likely to be weakened by the oxidation of carbon leading to reduced load transfer from the matrix to the fibres.

The plateau for the high mechanically applied stresses is set by the saturation matrix crack spacing, which is a function of the transfer length for shedding the load back from the fibres to the matrix. For the same thermally applied stress levels the temperatures are greater than 800°C and silica bridges are expected to form between the fibre and matrix. It is suggested that this observed effect may be attributed to the increased strength of the interphase requiring an increase in applied stress to initiate cracks; these cracks occur, therefore, where the fibres are weakest and crack spacing is more dependent on the fibre properties.

In addition to possible interfacial effects discussed above there may be an effect due to a variation in " A ", as a result of a change in the heat transfer rate between the hot sample and the quenching medium, which may contribute to the apparent different response of the

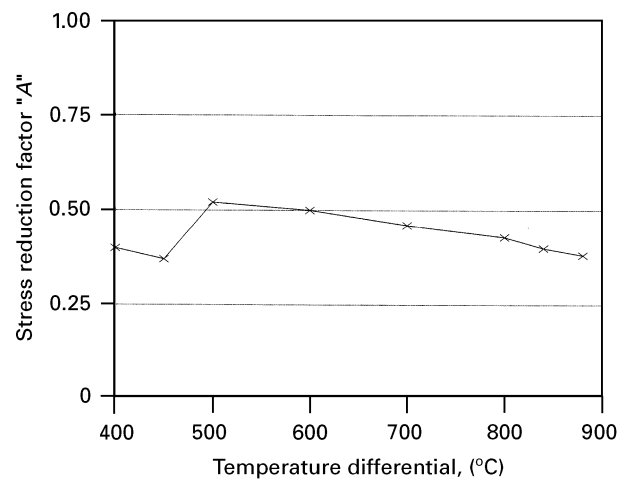


Figure 5 Variations in stress reduction factor with severity of thermal shock in water quench test.

material to mechanically or thermally applied stresses. As shown by the data in Fig. 4 the crack density produced by a total matrix axial stress of 210 MPa was the same whether produced by mechanical means [7] or generated thermally, as in this study, by shocking the samples with a temperature differential (ΔT) of 600°C and taking A to be 0.5. By comparing other crack densities produced in these investigations the apparent variation in the stress reduction factor can be calculated to enable the total matrix stress applied thermally (thermal shock + residual thermal stress) to be equated with the mechanically applied plus residual stress. There is a clear trend in the variation of values for " A " with thermal shock temperature differential as shown in Fig. 5. Comparison with the work of Singh *et al.* [25] reveals a possible trend from a nucleate boiling regime at low temperatures to one in which a film of steam envelopes the sample, progressively reducing the heat transfer rate, at higher temperatures. It is proposed, therefore, that a complex relationship exists between crack density and thermally induced modifications to interfacial properties and/or a change in the heat transfer rate with severity of thermal shock.

6.2.2.3. Prediction of cracking damage perpendicular to the fibre direction. (i) Determination of maximum temperature differential. The model of Aveston *et al.* [1] for determining the initiation of matrix cracking in a fibre-reinforced brittle matrix composite is used in an attempt to predict the maximum permissible operating temperature before matrix cracking of the unidirectional Nicalon reinforced CAS material would occur under thermal shock conditions. The relationship between matrix cracking strain (ϵ_{mu}) and material properties was given as:

$$\epsilon_{\text{mu}} = \left[\frac{12\tau\gamma_m E_f V_f^2}{E_c E_m^2 r V_m} \right]^{1/3} \quad (4)$$

where E is Young's modulus, V is the volume fraction, r is the fibre radius, τ is the interfacial shear stress and

γ is the fracture surface energy; m, f and c refer to the matrix, fibres and composite respectively.

Downward thermal shocks apply tensile stresses to the surface of the material and Equation 4 can be converted to matrix stress values simply by using the relationship $\sigma_{\text{mu}} = E_m \varepsilon_{\text{mu}}$ to give:

$$\sigma_{\text{mu}} = \left[\frac{6\tau\Gamma_m E_f E_m V_f^2}{E_c r V_m} \right]^{1/3} \quad (5)$$

where $\Gamma_m (= 2\gamma_m)$ is the matrix fracture energy.

The level of stress to cause matrix cracking should be the same whether applied mechanically or thermally, hence its value can be equated with a temperature differential via Equation 2. However, residual stresses within the composite must also be included. At the onset of matrix cracking $\sigma_{\text{mu}} = \sigma_{\text{ts}} + \sigma_r$ hence, by combining and rearranging Equations 2 and 5 an expression for the maximum temperature differential (ΔT) can be obtained:

$$\Delta T = \frac{1 - \nu}{AE_m \alpha_m} \left[\left(\frac{6\tau\Gamma_m E_f E_m V_f^2}{E_c r V_m} \right)^{1/3} - \sigma_r \right] \quad (6)$$

where A is 0.5 and σ_r is the residual matrix axial stress at the thermal shock temperature. The remaining terms that have not been determined experimentally are the interfacial shear stress (τ) and the matrix fracture energy (Γ_m). Therefore, if values for A, τ and Γ_m can be determined independently, it may be possible to predict the maximum operating temperature from Equation 6.

(ii) Determination of interfacial shear stress. A variety of techniques have been employed in attempting to determine the interfacial shear stress (τ) in the Nicalon/CAS composite. From a recent report [29] it is clear that there is a large spread of values (3.5–19 MPa) but the majority fall within the range 10–15 MPa. The experimental method used to determine τ in this project was to measure the saturation crack spacing after the composite had been subjected to axial tensile stresses generated during flexure testing. The procedure for crack measurement and calculation of interfacial shear stress was similar to that reported previously [7]. An estimation of the value of interfacial shear stress, τ , can then be made using the relationship:

$$\tau = \frac{V_m \sigma_{\text{mu}} r}{V_f 1.5 S_f} \quad (7)$$

where r is the fibre radius, S_f is the saturation crack spacing and σ_{mu} is the total matrix cracking stress (obtained from the onset of non-linear behaviour in flexure tests [30]). The results were in agreement with the suggestion that moderate increases in the severity of thermal treatments leads to lower values of τ , although the calculated value of 24 MPa for the as-received material appears high. However, since σ_{mu} values obtained from flexure tests are higher than from tensile tests, τ values are also expected to be higher, although the rankings should be correct.

(iii) Determination of matrix fracture energy. An indentation approach to determining the fracture energy of the CAS was chosen for this project since there was only a small amount of material available. Following the approach of Chantikul *et al.* [31] the stress intensity factor (K) is given by:

$$K = \eta \left(\frac{E}{H} \right)^{1/8} (\sigma_{3b} P_i^{1/3})^{3/4} \quad (8)$$

where η is a geometric constant ($= 0.59 \pm 0.12$), E is Young's modulus, H is the hardness, σ_{3b} is the applied stress and P_i is the indenter load. The hardness of the monolithic CAS can be obtained from the relationship:

$$H = \frac{P_i}{\alpha_0 a_i^2} \quad (9)$$

where α_0 is a geometric constant ($= 2$ for Vickers indenters) and a_i = half the length of the indentation impression diagonal. An expression for the critical stress intensity factor (K_c) could then be obtained by combining Equations 8 and 9 to give:

$$K_c = \eta \left(\frac{E \alpha_0 a_i^2}{P_i} \right)^{1/8} (\sigma_{3b} P_i^{1/3})^{3/4} \quad (10)$$

Values obtained from tests using an indentation load of 19.6 N are shown in Table III. The mean value for the hardness of the monolithic material (8.2 GPa) is in close agreement with a value of 8.4 GPa obtained by Anstis *et al.* [32] for a glass-ceramic, although values for the critical stress intensity factor were, generally, a little lower than the quoted value of 2.5 MPa m^{1/2} [32] for a glass-ceramic tested using the double cantilever beam method.

The fracture energy (Γ_m) may then be determined from the relationship:

$$\Gamma_m = \frac{K_c^2 (1 - \nu^2)}{E} \quad (11)$$

A fracture energy value of approximately 46 J m⁻² was calculated by using a mean value of 2.1 MPa m^{1/2} for the stress intensity factor and this is above the top end of the range of 15–40 J m⁻² that is usually cited in the literature as being representative of fracture energies for glass-ceramics [6, 26].

An alternative method requiring the measurement of the depth of crack produced by the indentation [33] led to a value of 36 J m⁻² for the fracture energy of monolithic CAS.

(iv) Validation of ACK model. By inserting values of interfacial shear stress (τ) and matrix fracture energy (Γ_m) into Equation 6 the validity of using the ACK relationship for calculating the cracking threshold and hence the most severe thermal shock to which the unidirectional Nicalon reinforced CAS may be subjected without cracking the matrix can be tested. The relationship between the different parameters is shown in Fig. 6, where the relative values of Γ_m for a range of values of τ is given for temperature differentials between 250–500 °C. The box represents limits obtained from the majority of values of interfacial shear stress given in reference [29] and a range of possible matrix fracture energies.

TABLE III Fracture energy of monolithic CAS obtained using a 19.6 N Vickers indenter

Load W (N)	Flexure strength σ_{3b} (MPa)	Indenter diagonal $2a$ (μm)	Hardness H (GPa)	Stress intensity K_c ($\text{MPa m}^{1/2}$)	Fracture energy Γ (J m^{-2})
56	155	66	9.0	2.3	56.5
72	126	72	7.6	2.0	41.2
78	135	74	7.2	2.1	45.9
72	131	66	9.0	2.1	43.8
77	141	70	8.0	2.2	49.0

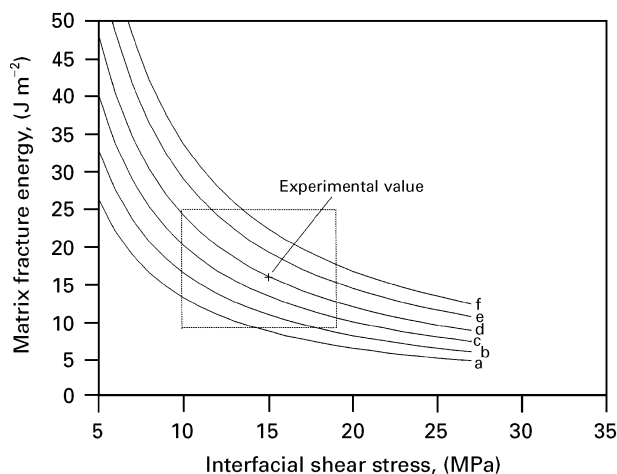


Figure 6 The relationship between interfacial shear stress and fracture energy for matrix cracking in Nicalon/CAS over a range of temperature differentials of (a) 250°C (b) 300°C, (c) 350°C, (d) 400°C (e) 450°C and (f) 500°C. Note: The experimental value refers to a combination of the interfacial shear stress (15 MPa) and the experimentally observed matrix cracking temperature.

The values of Γ_m , however, are not the values often quoted for glass-ceramics and are lower than those measured for the bulk matrix material used in this work. The upper limit of 25 J m^{-2} is set by values reported by other research groups for monolithic CAS material and the lower limit of 9.5 J m^{-2} is that reported by Curtin [34] in which the experimental data on multiple matrix cracking obtained by Beyerle *et al.* [6] was used to calculate the interfacial shear stress, τ , thus enabling a value for Γ_m to be inferred from the ACK model.

Matrix cracking was observed at a temperature differential of 400°C and a value for the interfacial shear stress at this temperature is assumed to be about 15 MPa (this is an average value for as-received material from reference [29]). These values, also shown in Fig. 6, indicate that for the modified ACK model to predict an accurate severity of thermal shock for the onset of matrix cracking in the unidirectional Nicalon/CAS a matrix fracture energy of approximately 16 J m^{-2} would be required. A reduction in the fracture energy from 25 J m^{-2} for the monolithic CAS material to 16 J m^{-2} for the matrix material may not be unreasonable since it should be noted that the fracture energies cited above were determined for monolithic CAS.

There are two possible reasons for the apparent lower energy required to fracture the matrix of the composite. Firstly, residual stress fields generated in the matrix of the composite become increasingly tensile as fibres are approached and secondly, microstructural changes occur. An even distribution of nucleating agent in the monolithic material is replaced by dispersion to grain boundaries in the composite which may result in a change to the fracture toughness.

Although more accurate determinations of interfacial shear stress and the fracture energy of the matrix material would be necessary to make a detailed comparison between ACK and experimental values for matrix cracking in the unidirectional reinforced composite, Fig. 6 indicates clearly the interaction between interfacial shear stress, fracture energy and the thermal shock temperature differential.

7. Conclusions

Two types of matrix cracking occur in the unidirectional composite when subjected to thermal shock, a single crack on the cross-sectional faces and multiple cracking perpendicular to the fibre direction. The frequency of cracks in the perpendicular direction was seen to be related to temperature, with the greatest crack density being observed at intermediate temperature differentials ($\Delta T = 550\text{--}750^\circ\text{C}$) and fibre fracture occurring only at temperatures above this level. Crack density data from thermal shock tests were correlated with similar crack patterns seen under mechanically applied tensile loading and appear consistent with changes to the interphase expected to occur in this type of composite at elevated temperatures.

A modified version of the ACK model is applicable to the determination of the critical temperature differential for the onset of matrix cracking providing values of some key parameters can be determined independently.

Acknowledgements

The authors would like to thank the EPSRC and DRA at Farnborough for financial support for this project through a CASE Award and Rolls-Royce plc. for provision of the experimental material. Drs G Harrison (DRA) and M Percival (Rolls-Royce plc) are thanked for their interest in and support of the project.

References

1. J. AVESTON, G. A. COOPER and A. KELLY, in *Proceedings of The National Physical Laboratory (IPC Science and Technology Press Ltd, London 1971)*, Paper 2, pp. 15–25.
2. D. B. MARSHALL and A. G. EVANS, *J. Amer. Ceram. Soc.* **68** (1985) 225.
3. K. M. PREWO, *J. Mater. Sci.* **21** (1986) 3590.
4. A. G. EVANS and D. B. MARSHALL, *Acta Metall.* **37** (1989) 2567.
5. R. Y. KIM and N. J. PAGANO, *J. Amer. Ceram. Soc.* **74** (1991) 1082.
6. D. S. BEYERLE, S. M. SPEARING, F. W. ZOK and A. G. EVANS, *ibid.* **75** (1992) 2719.
7. A. W. PRYCE and P. A. SMITH, *J. Mater. Sci.* **27** (1992) 2695.
8. *idem*, *Acta Metall. Mater.* **41** (1993) 1269.
9. S. M. SPEARING, F. W. ZOK and A. G. EVANS, *J. Amer. Ceram. Soc.* **77** (1994) 562.
10. R. F. COOPER and K. CHYUNG, *J. Mater. Sci.* **22** (1987) 3148.
11. R. J. KERANS, R. S. HAY, N. J. PAGANO and T. A. PARTHASARATHY, *Ceram Bull* **68** (1989) 429.
12. E. BISCHOFF, M. RÜHLE, O. SBAIZERO and A. G. EVANS, *J. Amer. Ceram. Soc.* **72** (1989) 741.
13. M. H. LEWIS and V. S. R. MURTHY, *Comp. Sci. and Tech* **42** (1991) 221.
14. S. M. BLEAY, V. D. SCOTT, B. HARRIS, R. G. COOKE and F. A. HABIB, *J. Mater. Sci.* **27** (1992) 2811.
15. Y. KAGAWA, N. KUROSAWA and T. KISHI, *ibid.* **28** (1993) 735.
16. J. J. BRENNAN and K. M. PREWO, *ibid.* **17** (1982) 2371.
17. T. MAH, M. G. MENDIRATTA, A. P. KATZ, R. RUH and K. S. MAZDIYASNI, *J. Amer. Ceram. Soc.* **68** (1985) C248.
18. E. Y. LUH and A. G. EVANS, *ibid.* **70** (1987) 466.
19. M. D. THOULESS, O. SBAIZERO, L. S. SIGL and A. G. EVANS, *ibid.* **72** (1989) 525.
20. M. W. PHAROAH, A. M. DANIEL and M. H. LEWIS, *J. Mater. Sci. Lett.* **12** (1993) 998.
21. K. P. PLUCKNETT and M. H. LEWIS, *ibid.* **14** (1995) 1223.
22. R. C. WETHERHOLD and L. P. ZAWADA, *J. Amer. Ceram. Soc.* **74** (1991) 1997.
23. W. R. BUESSEM, *ibid.* **38** (1955) 15.
24. D. P. H. HASSELMAN, *ibid.* **53** (1970) 490.
25. J. P. SINGH, Y. TREE and D. P. H. HASSELMAN, *J. Mater. Sci.* **16** (1981) 2109.
26. C. M. A. DAVIES, B. HARRIS and R. G. COOKE, *Composites* **24** (1993) 141.
27. R. W. DAVIDGE “Mechanical Behaviour of Ceramics” (Camb. Univ. Press, Cambridge 1979).
28. K. L. POWELL, P. A. SMITH and J. A. YEOMANS, *Compos Sci and Tech* **47** (1993) 359.
29. E. LARA-CURZIO and M. K. FERBER, *J. Mater. Sci.* **29** (1994) 6152.
30. M. J. BLISSETT Ph.D thesis, University of Surrey, (1995)
31. P. CHANTIKUL, G. R. ANSTIS, B. R. LAWN and D. B. MARSHALL, *J. Amer. Ceram. Soc.* **64** (1981) 539.
32. G. R. ANSTIS, P. CHANTIKUL, B. R. LAWN and D. B. MARSHALL, *ibid.* **64** (1981) 533.
33. A. S. KOBAYASHI, M. ZII and L. R. HALL, *Int. J. Fract. Mech.* **1** (1965) 81.
34. W. A. CURTIN, *Acta Metall. Mater.* **41** (1993) 1369.

*Received 19 April
and accepted 21 May 1996*